Materials Advances

ROYAL SOCIETY OF CHEMISTRY

PAPER

View Article Online
View Journal | View Issue

Open Access Article. Published on 20 October 2022. Downloaded on 1/18/2026 10:53:13 AM.
This article is licensed under a Creative Commons Attribution-NonCommercial 3.0 Unported Licence.

Check for updates

Cite this: *Mater. Adv.*, 2022, 3, 9040

# Graphene oxide-incorporated cementitious composites: a thorough investigation

Ali Bagheri, Ehsan Negahban,* Ali Asad, Haider Ali Abbasi and Syed Muhammad Raza

Received 14th February 2022,
Accepted 19th October 2022

DOI: 10.1039/d2ma00169a

rsc.li/materials-advances

The use of nanomaterials, particularly carbon-derived ones, has always been a high-tech topic of research in the field of cement and concrete. Graphene and its derivatives are the most popular carbon-based nano-additives in cementitious composites. Although the literature covers many aspects of this field, the existence of comprehensive research on physical, mechanical and durability-related characteristics of graphene oxide (GO)-incorporated cement composites is required. This study scrutinises flowability, flow loss, setting time, ultrasonic pulse velocity, electrical resistivity, compressive strength, flexural strength, water sorptivity, apparent density and volume of permeable voids (VPV) of cement composites reinforced by 0.01 wt% to 0.5 wt% GO by weight of cement. The results indicated that using GO reduced the initial setting time by 9–23% and flowability by up to 31%. While the electrical resistivity of GO-incorporated specimens was higher than the normal cementitious composites, the highest resistivity was achieved in a specimen with 0.05% GO. The transmitted pulse velocity through the specimens showed that despite a reduction in specimen with 0.01% GO, the UPV of other specimens was above 4 km $s^{-1}$, displaying a good structural quality and homogeneity. A noticeable improvement of up to 28% and 50% in compressive and flexural strength was witnessed with the addition of GO. Moreover, the inclusion of GO significantly improved transport properties as it lowered the VPV and water sorptivity by up to 15% and 66%, depending on the added percentage of GO.

## 1. Introduction

The service life of a building and its load-bearing capacity mainly depends upon durability and strength. Structures' service life is identified as the duration under which it can sustain an acceptable and safe performance level, keeping in view all the environmental restraints.[1,2] The exponential growth of the construction industry in the past few decades has demanded new ways and techniques to cope with strength and durability issues to increase the service life of the structures.[3] Ordinary Portland cement (OPC)-based concrete is a heterogeneous material with a porous microstructure. This porosity makes the OPC concrete vulnerable to chemical attacks, weathering conditions, and other service-life challenges.[4]

Three types of pores exist in concrete: (1) air pores, which are formed due to the entrained air. A vibration device is used to reduce air pores in concrete. These vibrations increase the local pressure of cement paste to reduce the friction among aggregates. (2) Capillary pores, in which the water/cement (W/C) ratio governs the changes. The lower the W/C ratio, the fewer will be the capillary pores. These pores can also be reduced using additives such as plasticisers and micro silica.[5] (3) Gel pores, which are embedded within the calcium silicate hydrate (CSH) microstructure of cement. Almost one-third of the pore space is comprised of gel pores.[6] These pores are due to the vacancies in the principal atoms and spaces between the network of layers.[7,8] The porosity of concrete is directly related to the strength and durability of concrete.[9–11]

The construction industry is an ever-growing industry with the tendency to move towards sustainability and optimisation. To cover this aim, researchers have focused on building more durable and stronger binders by improving the physical, mechanical, microstructural, and transport properties of cementitious composites utilising different approaches.[2,12–21] The ease with which liquids and gases can enter the cementitious network represents its transport properties.[22] Transport properties include water permeability, gas permeability, water sorptivity and chemical resistance. Over the years, fibre additives such as steel and polymer fibres were explored in the initial phase of investigations. These additives convincingly improved the mechanical properties of concrete. The addition of fibres such as polypropylene to reinforced concrete significantly enhanced the compressive and tensile strength.[23] However, the microstructure and porosity did not change much as

*Department of Civil and Construction Engineering, Faculty of Science, Engineering and Technology, Swinburne University of Technology, Melbourne, Australia.*
*E-mail: enegahban@swin.edu.au*


© 2022 The Author(s). Published by the Royal Society of Chemistry

Open Access Article. Published on 20 October 2022. Downloaded on 1/18/2026 10:53:13 AM. This article is licensed under a Creative Commons Attribution-NonCommercial 3.0 Unported Licence.

these additives could not fill pores at the micro-level.[24–26] To improve the porosity of cementitious composites at the micro/nano level, nanomaterials have found great importance in advanced research.[27]

Nanomaterials can be classified into three types based on their shapes and spatial organisation.[28] The types are zero-dimensional (0-D) particles, one-dimensional fibres and two-dimensional sheets.[29–31] Nano $SiO_2$, as a 0-D additive, is extensively used to enhance the workability and water penetration resistance of concrete. It also helps calcium leaching, which adversely affects the durability of concrete.[32] This enhancement in the aforementioned features is due to the nucleation effect, which involves filling the pores in the concrete structure. Moreover, There is no crack-bridging effect in 0-D nanoparticles as they have a spherical shape.[33,34]

Cement composites also depicted higher chloride penetration resistance after adding 1% nano-silica.[35] Du *et al.*[36] reported that adding 0.3% nano-silica can reduce 45%, 28.7% and 31% of water penetration, chloride migration, and diffusion coefficient, respectively, in concrete. The positive impacts of incorporating nanomaterials in cementitious composites were observed in other studies as well.[37–39] The addition of nano-montmorillonite and nano-titanium to the cement mortar increased the 28 day compressive and flexural strength by 15% and 13%, respectively. Moreover, the compressive strength gain in the early stages improved notably due to the cement hydration acceleration caused by the high specific surface of nanomaterials. Due to their filling properties and crack-bridging nature, a denser microstructure and hydration products were formed when nanomaterials were added.[40] Reviewing the literature implied that while mechanical and microstructural improvements can be achieved by incorporating nanomaterials, finding the optimum replacement percentage requires considerations.[39–41]

Carbon nanotubes (CNTs) are another type of revolutionary nano reinforcement, which has opened new possibilities for strengthening cementitious materials.[42] CNTs, as 1-D nano-reinforcement agents, have significantly high Young's modulus, tensile strength, and lateral size-to-thickness ratios.[43–47] CNTs possess strong van der Waals forces, which tend to form CNT bundles.[48] In studies conducted on CNT-reinforced cement composites, it was concluded that incorporating CNTs can accelerate the hydration process and improve mechanical strength.[49–51] The main mechanism in CNT-incorporated cement composites was found to be the nucleation effect, which helped fill up the gaps pertaining to micro-sized capillary pores. Furthermore, The crack-bridging, pull-out and filling mechanisms of CNTs were found to be beneficial for producing a more compacted and denser microstructure by filling the existing voids between CSH products and improving the mechanical properties of cementitious composites.[50]

On the other hand, in a study performed on cementitious composites under the influence of multi-walled carbon nanotubes (MWCNTs), it was reported that MWCNTs showed weak bonding with the cement matrix due to sliding.[52] Because of the poor dispersion and weak bonding of the cement matrix with CNTS, the influence of CNTs on the properties of cementitious composites and their efficacy is restricted. However, the mentioned challenges can be resolved by utilising CNTs, nanoparticles and surfactants simultaneously. The combined effects of nano-filling capability, providing more nucleation sites, and geometric properties of nanoparticles, alongside the crack-bridging effect of CNTs, were deemed to improve the mechanical strength.[53] It is worth noting that for the optimum efficacy of CNTs, certain influential parameters, including the type, incorporating volume, dispersion method, and water-to-cement and sand-to-cement ratios, must be considered.[53–56]

The advancement in nanomaterials technology has found an extraordinary nano-sized additive for cementitious materials called graphene oxide (GO). GO has exhibited major improvement in the properties of concrete, including significant changes in the microstructure.[57] GO is formed by the oxidation of graphite, a material comprised of three-dimensional carbon atoms organised as a layered structure of carbon atoms connected to the oxygen functional groups. These functional groups separate the layers of carbon atoms and make them hydrophilic (tendency to dissolve in water easily).[58] It was found that ultrasonication can exfoliate this layered structure and enhance the dispersion.[59] If the carbon atoms have one or few layers, these exfoliated sheets can be termed GO.[60] It consists of various layers with hydrophilic oxygenated sheets of graphene incorporating the carbonyl and carboxyl groups at the surface, while hydroxyl groups are located at the base.[61,62] GO is a hydrophilic material because carbon atoms have $sp^2$ and $sp^3$ hybridised orbitals forming a hexagonal microstructure. The hydrophilic tendency of GO gives it an edge over CNTs and graphene.[62] The microstructure of GO sheets constitutes a rough surface because of the covalently bonded functional groups present in its microstructure.[63,64] GO possesses excellent mechanical properties and a high aspect ratio, with an elastic modulus of 23–42 GPa[27] and tensile strength of around 130 MPa.[31,64]

Another benefit of using GO is that it can be obtained in large quantities from an inexpensive source (graphite powder), making it an ideal material to be used in cement composites. This gives GO the benefit over 0-D nanoparticles and 1-D nanotubes for utilisation with improved rheological, mechanical, and transport properties. Furthermore, GO provides an additional dimension of interaction with the cementitious network. These benefits of GO over other nano reinforcement agents make it a distinct potential candidate for future research in this domain.

Many researchers have identified that using GO affects cement composites' physical and mechanical properties. Workability is one of the challenges that is generally compromised in graphene-incorporated cement pastes.[65] Shang *et al.*[66] investigated the rheological behaviour of cement paste incorporating GO and found that adding GO decreased the fluidity of the cement mix. A 21% reduction was also observed by incorporating 0.03 wt% GO in the cement paste.[67] This reduction in fluidity can be connected to the high concentration of agglomerates due to the electrostatic attraction between GO and the

Open Access Article. Published on 20 October 2022. Downloaded on 1/18/2026 10:53:13 AM.
This article is licensed under a Creative Commons Attribution-NonCommercial 3.0 Unported Licence.

cement paste.[67] The agglomerates and flocculation could be broken by shear mixing since they were unstable. A further reduction of 41.7% in workability was observed when 0.05% of graphene oxide was added.[68] Several researchers have found that the hydrophilic groups in graphene oxide have a large surface area and strong water-absorption capacity. Because of that, the free water content is reduced, resulting in increased frictional resistance among cement particles.[31,68,69] Water-reducing admixtures and superplasticisers are generally used to improve the workability of cementitious composites incorporating graphene oxide.[70,71]

Despite the drawbacks of using GO on the rheological and workability properties of cementitious composites, its significant improvement in mechanical properties is undeniable. Lv *et al.*[72] studied the effects of GO incorporation in cementitious composites. They reported 160%, 197.2%, and 184.5% increases in compressive, tensile, and flexural strength, respectively, by adding 0.02% GO by weight of cement. Pan *et al.*[31] concluded that adding 0.05% GO to the cementitious composites can lead to a 15–33% and 41–59% increase in compressive and flexural strength. Furthermore, elastic modulus increased up to 500% with the addition of 3% GO by weight of cement.[73] Superior mechanical properties of GO, acceleration of cement hydration through seeding effects of GO, densification of the microstructure, filling pores and reducing porosity, and optimising the microstructural bonding, are among the reasons that contributed to the enhancement of mechanical properties of cement composites.[31,68,71,73–76]

Various studies were conducted with the hypothesis that nano-sized additives could improve the microstructure of cement binders by reducing their permeability.[27,75,77–80] The improved permeability of the binders makes them more resistant to chemical attacks and fluid ingress. The durability has a direct relation with the transport properties of cementitious composites.[1] Total porosity, pore size distribution, pore connectivity and tortuosity are among the key factors governing cementitious composites' transport properties.[81] Water sorptivity is one of the significant indexes of concrete durability.[82,83] The governing force of water ingress during the sorption process is the internal capillary pressure.[84] Subsequently, increased water penetration resistance enhances concrete's durability.[1,85] The chemical ingress is also due to the porosity of concrete and its transport characteristics. Certain efforts have been made to investigate this aspect of transport properties using different nanomaterials like nano-silica, CNTs, and GO. The increase in chloride penetration resistance of the GO-incorporated cement paste was observed by Indukuri and Nerella[2] when the depth of chloride penetration was reduced between 15 and 40% for various percentages of added GO.

The findings of previous studies indicated that incorporating GO in cementitious composites is sensitive to the GO content within the mix design. The research on finding an optimum GO content for cementitious composites revealed that the inclusion of GO in higher dosages could result in fluctuation of properties. Li *et al.*[86] stated that the incorporation of GO improved cement's mechanical properties. However, the flexural strength experienced a decline when more than 0.04 wt% GO was added to the paste. A similar fluctuation was witnessed in electrical resistivity, especially when the GO content was more than 0.04 wt% The adverse effect could to attributed to GO agglomeration at higher contents.[86–88]

It is imperative to understand that most of the research activities in this field have focused separately on certain characteristics. To assess the suitability of GO and its impacts on various properties, the need for a thorough and conclusive investigation of a uniform and consistent cementitious mixture is still felt. Additionally, the effects of GO on the properties of cement binders vary at different fractions, which opens a research gap for further investigation in this field. This study conclusively investigates the physical, mechanical, and transport behaviour and properties of cementitious composites incorporated with 0.01%, 0.03%, 0.05%, 0.1%, 0.3%, and 0.5% GO by weight of cement.

## 2. Experimental procedure

### 2.1. Materials

To prepare the GO-incorporated cement composites, a commercially available Bastion general purpose (GP) cement in compliance with AS3972 was used.[89] Natural river sand with a particle size distribution between 50 μm and 4.75 mm was utilised as the fine aggregate to prepare the cement mortar. GO powder was employed to prepare a distilled water-dispersed GO aqueous suspension *via* sonication.[90] The characteristics of as-received GO nanoplates are shown in Table 1.

### 2.2. Mixture preparation

The GO aqueous suspension was prepared prior to mortar preparation. The addition of GO to distilled water was according to the mass quantities calculated based on the mixture proportions shown in Table 2. An ultrasonic cell crusher chamber was used for this purpose. The required amount of GO nanosheet powder mixed with 200 ml of water was placed in a flask. The sonication chamber was set to operate for two minutes, and the flask was removed afterwards. The water-to-cement (w/c) ratio used throughout the experimental phase was fixed at 0.45.

A Hobart mortar mixer was utilised to prepare the GO-incorporated cement mortars. Calculated quantities of cement and sand, based on Table 2, were dry-mixed in the mixing bowl for 30 seconds. The dispersed GO solution and the remaining required water were then added to the mixing bowl and mixed for 5 minutes to produce a homogeneous mortar. The mortar was poured into the specified moulds and vibrated for 30 seconds on the vibration table to ensure uniform compaction

Table 1 Properties of GO nanosheets

| Properties | Purity (%) | Density (kg m$^{-3}$) | Aspect ratio | Surface area (m$^2$ kg$^{-1}$) |
|---|---|---|---|---|
| Values | 99.9 | $2.2 \times 10^3$ | 1000 | $3.5 \times 10^5$ |

 © 2022 The Author(s). Published by the Royal Society of Chemistry

Open Access Article. Published on 20 October 2022. Downloaded on 1/18/2026 10:53:13 AM.
This article is licensed under a Creative Commons Attribution-NonCommercial 3.0 Unported Licence.

Table 2 Mix design of GO-based cement composites

| Sample designation | Cement : sand | W/C | GO wt% to cement |
|---|---|---|---|
| C0[a] | 1 : 1.5 | 0.45 | 0 |
| C1 | | | 0.01 |
| C3 | | | 0.03 |
| C5 | | | 0.05 |
| C10 | | | 0.1 |
| C30 | | | 0.3 |
| C50 | | | 0.5 |

[a] Control sample without GO.

and removal of air bubbles. The moulds were wrapped with polyethylene sheets to prevent the rapid evaporation of water and left for 24 hours at room temperature of 23 ± 2 °C, followed by a water bath curing for up to 28 days for testing purposes.

### 2.3. Testing procedures

The experimental programme of this study assessed the three aspects physical, mechanical, and durability (transport) of specimens as described below.

#### 2.3.1. Physical observations

*(A) Flowability and flowability loss.* These tests determine the consistency of the cement mortar and identify the transportable moisture limit. A flow table was used to perform the flowability and flowability loss tests of the fresh cement mortar. The test was carried out in accordance with ASTM C1437.[91] The formula presented in eqn (1) is used to calculate the flow rate of mortar.

$$\text{Flow rate} = \left[\frac{(D_{\text{avg}} - D_0)}{D_0}\right] \times 100 \quad (1)$$

where $D_0$ is the average diameter of the specimen before 25 blows and $D_{\text{avg}}$ is the average diameter of specimens after 25 blows. For flow loss, the same procedure was repeated every 30 minutes until the flow rate change was reduced to zero.

*(B) Setting time.* The initial setting time of the paste was measured using the Vicat needle test in accordance with ASTM C191.[92] The initial setting time refers to the time when cement paste starts losing its plasticity.[93] If the initial setting time of cement is $X$ minutes, the mortar should be placed in the desired position within $X$ minutes of adding water. The mortar will lose its optimum strength if the process is delayed.

*(C) Ultrasonic pulse velocity (UPV).* The UPV is a non-destructive test (NDT) generally used to identify the voids, cracks and damages to the material and assess its quality by measuring the velocity of the ultrasonic pulses transmitted through the specimen.[94] The test was performed following ASTM C597[95] after 7 days of curing. A Matest UPV tester with two 55 kHz cylindrical transducers was used to measure the time that the pulse travelled through the specimens. The UPV, subsequently, was calculated using the formula shown in eqn (2).

$$\text{UPV} = \frac{L \times 10^3}{T} \quad (2)$$

where $L$ is the distance in mm, $T$ is the time in μs, and UPV is in km $s^{-1}$.

*(D) Electrical resistivity.* The electrical resistivity of the specimens was measured in accordance with ASTM C1876[96] using a Resipod device after 7 days of curing. Resipod is an integrated 4-point probe and a non-destructive method of measuring resistivity. The electrical resistivity determines the correlation between the resistivity and chloride diffusion rate.[97] Moreover, the rate of concrete corrosion can be measured using this method.

#### 2.3.2. Mechanical properties

*(A) Compressive strength.* For each set of GO-incorporated cement mortars, six cylindrical specimens with 50 mm radius and 100 mm height were cast and tested according to ASTM C39[98] after 7 and 28 days of curing. The average values of three specimens for each test were calculated to analyse the results. A 300 kN Tecnotest compression machine was used to conduct the experiments at a loading rate of 0.30 MPa $s^{-1}$.

*(B) Flexural strength.* A 50 kN MTS machine was utilised to conduct a three-point bending flexural test on 160 × 40 × 40 mm prisms in accordance with ASTM C348[99] after 7 and 28 days of curing. The flexural strength of specimens was calculated using the formula presented by eqn (3).

$$f_{\text{f}} = \frac{3PL}{(2bd^2)} \quad (3)$$

where $f_{\text{f}}$ is the flexural strength in MPa, $P$ is the maximum load in $N$, and $L$, $b$, and $d$ are, respectively, length, width and depth in mm.

#### 2.3.3. Transport behaviour

*(A) Water sorptivity.* The water sorptivity test has been designed to determine the water absorption rate of the cement mortar or concrete. This is done by exposing one side of the specimen to water and measuring the change in the mass due to water absorption over time. The test setup is illustrated in Fig. 1. When the specimens are exposed to water, the capillary suction gets domination due to the water ingress of unsaturated cement mortar. The water sorptivity test also determines the rate of water absorption at the surface, as well as the interior of cement mortar specimens, and was carried out according to ASTM C1585.[100]

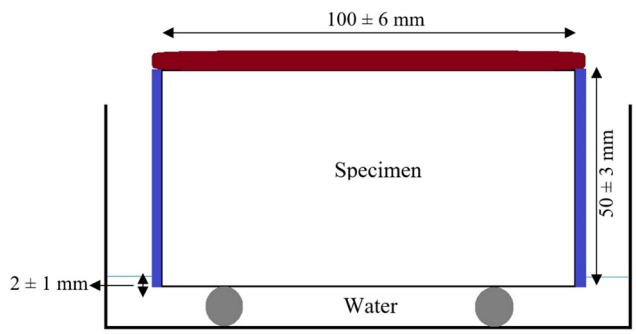


Fig. 1 Water sorptivity test setup.

Open Access Article. Published on 20 October 2022. Downloaded on 1/18/2026 10:53:13 AM.
This article is licensed under a Creative Commons Attribution-NonCommercial 3.0 Unported Licence.

*(B) Density and volume of permeable voids (VPV).* Density, water absorption and the volume of permeable voids are the key attributes of cement mortars evaluated by this test. The VPV test is a suitable method to investigate the porosity of cementitious composites as an important input for assessing the durability of mortars and concretes. The density and VPV tests have been performed according to ASTM C642.[101]

# 3. Results and discussion

## 3.1. Physical properties

The initial setting time of the six GO-incorporated and the control specimens were recorded and presented in Fig. 2. The initial setting time is an important factor to measure due to its direct relationship with the nucleation phenomena, as one of the most significant effects of GO nanoplates on cementitious composites during the hydration process.

As Fig. 2 shows, the initial setting time of cement mortars varies from 250–330 min. It can be seen that the setting time decreases from 330 min in the control sample to 300 mm in sample C1 with 0.01% GO addition. This decline continues until 255 min in sample C5 with 0.05% GO. However, retaining the addition of GO gradually increases the cementitious composites' setting time back to 300 min until it plateaus in C30 with 0.3% GO nanoflakes. Since all the mixtures were set in more than 250 min, a flowability assessment of mortars from 0 to 150 min was done while mortars were in the fresh elastic phase. Fig. 3 demonstrates the fluctuations in the flow of the GO-incorporated cement composites over time, known as flow loss.

GO nanoflakes start influencing the cementitious matrix from the early stages of the fresh binder. The effects of GO on cement composites are derived from its exceptionally high surface area, which is about $3.5 \times 10^5$ $m^2$ $kg^{-1}$, compared to cement particles of about 400 $m^2$ $kg^{-1}$. This large surface area of GO nanosheets provides excellent nucleation sites with high energy levels for the precipitation of hydration products. Consequently, the addition of GO nanoplates greatly affects the initial setting time of cement composites. As depicted in Fig. 2, the addition of 0.05 wt% GO to cement mortar reduces the initial setting time by 23%, from 330 min to 255 min. Previous research[86,102] has confirmed that the heat of hydration (HoH) of cementitious binders is considerably influenced by the addition of GO, which creates an obvious link between these observations. An increase in the HoH of cement composites as a result of the GO inclusion can lead to a faster setting time. Apart from that, Li *et al.*[86] reported that a sample containing 0.04% GO reached the main hydration peak sooner than 3.5% GO containing sample, indicating that both induction and acceleration periods of the hydration process were accelerated by adding GO.

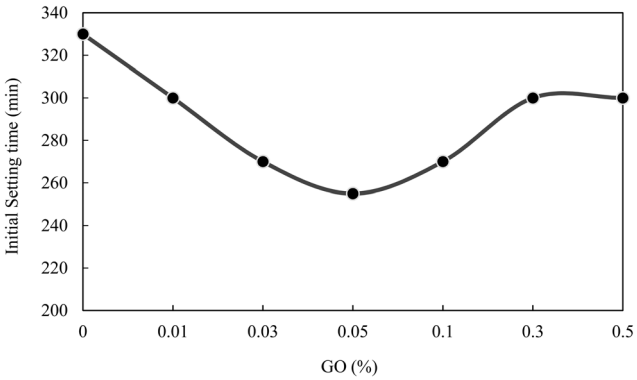


Fig. 2 Initial setting time of cement mortars.

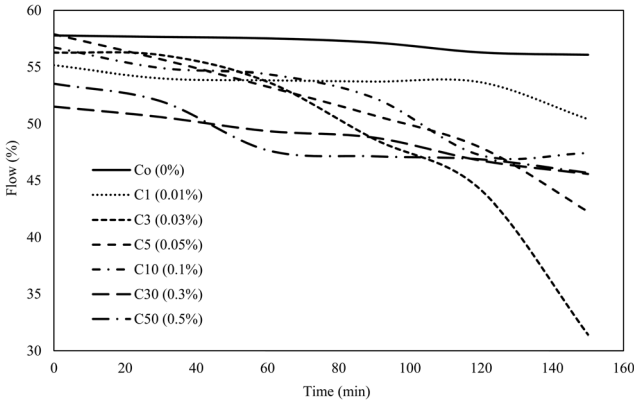


Fig. 3 Evolution of flowability of cement composites over time.

Additionally, another phenomenon also adversely affects the setting time as the content of GO increases. An increasing trend in the initial setting time and reaching back to 300 min is observed when GO content exceeds 0.05 wt%. The initial setting time of cement relies on the duration of the induction period in the evolution of HoH. Additionally, the duration of the induction period is a function of the diffusion rate of calcium ions from cement particles to the aqueous phase. This diffusion rate will be hindered if GO nanosheets are adsorbed on the surface of cement particles.[67] The addition of excessive GO (*i.e.*, more than 0.05 wt%) leads to the absorption of GO nanoflakes to the surface of cement particles, increasing the initial setting time.

The inclusion of GO nanoflakes in the composition of cement binders disturbs the rheological behaviour of binders as well. Changes in the rheological behaviour of GO-incorporated cement composites are evident in Fig. 3. It is noted that the flow loss of the control sample over the measurement time is minimum, and the flow loss occurred during the addition of GO. However, the highest loss of flowability was witnessed in the sample with 0.03 wt% GO. The change in the flow loss with the variation of GO illustrated the importance of GO content inclusion.

Fig. 3 reveals how the addition of GO nanosheets affects the flowability of cement mortars during their elastic state period. This function is an important rheological parameter of cement and concrete composites. As seen in this chart, the control sample maintains an almost constant flow during its elastic state, meaning no/negligible loss in the flow of mortar. Cement mortar containing 0.01% GO experiences a noticeable decline in the flow over time. The loss in the flowability of mortars

 © 2022 The Author(s). Published by the Royal Society of Chemistry

Open Access Article. Published on 20 October 2022. Downloaded on 1/18/2026 10:53:13 AM.
This article is licensed under a Creative Commons Attribution-NonCommercial 3.0 Unported Licence.

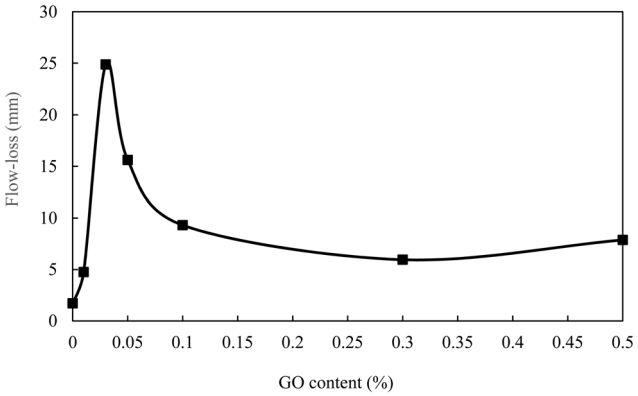


Fig. 4 Changes in flow-loss *vs.* GO content.

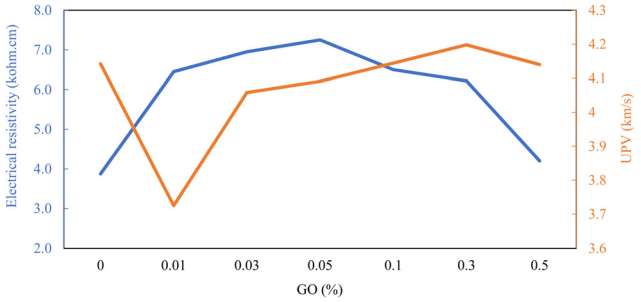


Fig. 5 Electrical resistivity and UPV results of GO-incorporated samples.

continues with the increase in the GO content up to 0.05%, with the most noticeable decrease occurring in sample C3, with 31.4% flow loss after 150 min. Moreover, the decrease in the flow of the cementitious composite reaches the maximum when 0.03 wt% GO is added and then declines as the GO content exceeds this limit, as can be seen in Fig. 4.

Reviewing the literature indicated that adding GO to cementitious composites can accelerate the hydration process and increase the heat of hydration, which can affect the fresh and rheological properties, including initial setting time, flowability, and flow-loss.[77,103] However, the highest impact of GO inclusion on fresh properties can be witnessed when the added GO is in the range of 0.03 wt% and 0.05 wt%. The observed results aligned with other studies suggesting the highest peak in the heat of hydration and subsequent impacts on fresh properties occurred in the same range of GO incorporation.[67,86] The flow loss of the samples, similar to the initial setting time, experiences fluctuations with the GO content. The flow loss of samples containing 0.1% GO nanoplates and above deems to be lower than samples with 0.03% and 0.05% GO.

The reduction in the flow of the cement mortar due to the addition of GO has been reported in previous research too.[31,66,68,104] This reduction could be due to GO nanoflakes' large surface area and their intensive hydrophilic characteristic.[105] As water is mixed with cement, GO nanoplates absorb the water molecules and reduce the workability. Furthermore, negatively charged graphene oxide particles can interact with the cement particles by electrostatic interaction and entrap a large amount of free water; hence, playing an important role in determining the rheological behaviour of cement composites.[27,66]

The results of electrical resistivity and UPV tests of the specimens, which are related to the structural integrity, flaws, and cracks, as well as voids and pore structure, are illustrated in Fig. 5. It is noticed from the chart that the addition of a maximum of 0.05 wt% GO to the cement mortar causes an increase in the electrical resistivity. Previous studies also observed and reported the increasing trend of electrical resistivity to a certain GO content followed by a reduction.[86,106]

Generally, there are two factors governing the electrical resistivity of cementitious binders, including the ion diffusion rate from cement particles to the aqueous phase, as well as ion transport within the cement matrix. On one hand, the introduction of GO nanosheets to the cement mortar accelerates the precipitation of hydration products. As the hydration process continues, the already-formed hydrates hinder the exposure of the solution to un-hydrated cement particles. Therefore, the electrical resistivity development is controlled by restricted ion diffusion due to the formation of thick hydrated barriers. On the other hand, the addition of more than 0.05 wt% GO to the system can increase the entrapped water molecules by these nanoplates leading to the facilitation of ion transport.[86] The observed fluctuation of electrical resistivity resulting from the increase of GO content was in good agreement with Li *et al.*,[86] in which the incorporation of 0.06 and 0.08 wt% GO resulted in a reduction of electrical resistivity.

UPV results of cement binders are mainly related to their structural integrity and cohesion. It is expected that the denser and more uniform the structure, the more the UPV. The existence of cracks, voids, entrapped air bubbles, *etc.*, may deteriorate the UPV of cement mortars. The findings obtained in this study confirm an increasing trend in UPV with the increase of GO content. However, the introduction of GO to the cement mortar significantly drops UPV. The increase of UPV with the increase of the GO content can be related to the higher dispersion of GO within the cement matrix, and filling the pores with large, nucleated surface area. The fluctuation of UPV with the addition of GO content was also witnessed in other studies and can be associated with the conflict of aforementioned factors and objects.[80,107,108]

### 3.2. Mechanical properties

Mechanical investigations, including compressive ($f_c$) and flexural ($f_f$) strength of the GO-incorporated cement mortars, are reported in Fig. 6 and 7, respectively. These figures illustrate not only the difference in strength caused by the addition of GO nanoflakes but also the strength development of GO-reinforced cementitious mortar.

Fig. 6 displays an increase in the $f_c$ of mortars as a result of GO addition. The $f_c$ increases from 23 MPa in the control sample after 7 days to a maximum of 33 MPa in the C3 mixture with 0.03% GO under the same curing conditions. This improvement in the $f_c$ continues in later stages where mixture C1 with 0.01% GO nanosheets develops 53 MPa strength,

Open Access Article. Published on 20 October 2022. Downloaded on 1/18/2026 10:53:13 AM.
This article is licensed under a Creative Commons Attribution-NonCommercial 3.0 Unported Licence.

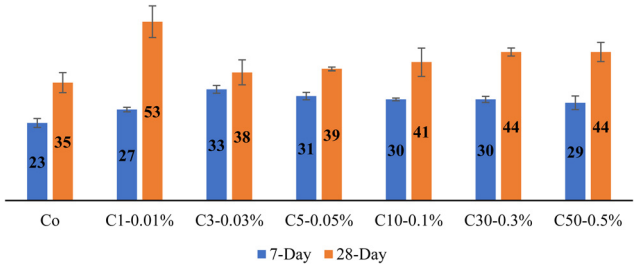


Fig. 6 Compressive strength (MPa) of GO-incorporated cement mortars.

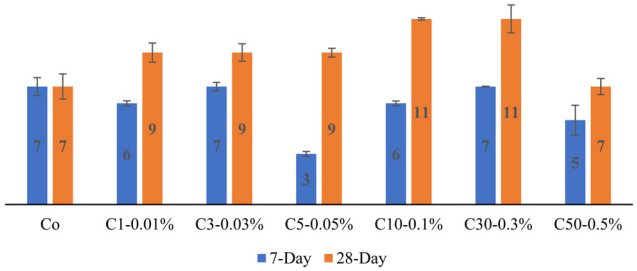


Fig. 7 Flexural strength (MPa) of GO-incorporated cement mortars.

notably higher than the control specimen with 35 MPa compressive strength after 28 days. Fig. 7 shows that the fluctuation of $f_f$, unlike $f_c$, is different in the early and late stages of curing. While no improvement is detected in 7 day $f_f$ due to the addition of GO nanoplates, the 28 day $f_f$ is positively affected by adding GO to all cement mortars.

Fig. 6 and 7 depict that the incorporation of GO nanoflakes influences the compressive/flexural strength of cement composites. However, this influence is not similar for flexure and compression at early and later stages. Adding GO to the cement mortars increases the compressive strength of samples by up to 43% in 7 days and up to 51% in 28 days. Nonetheless, GO declines flexural strength in the early stages (7 days) while it enhances the 28 day flexural strength by up to 57%. The strength improvement in GO-reinforced cement composites can be due to structural refinement. The existence of nucleated GO nanosheets can fill the pores within the matrix and decrease the volume of the large pores, as observed in other studies as well.[67,68] Obtaining a more homogeneous cementitious matrix can lead to strength gain. The strength gain mechanism, however, can be different for compression and bending. In bending, apart from structural integrity, the governance of the crack bridging role of GO nanosheets, which would develop in later stages (as the hydration process progresses), improves the 28 day flexural strength.

To obtain a better understanding of the effects of GO on the strength development of cement composites, the strength improvement is illustrated in Fig. 8. This figure visualises the strength development (compressive and flexural separately) from 7 to 28 days as a function of GO content. It can be noted that the strength development of GO follows a similar trend in compression and flexure. Regardless of the GO content, a

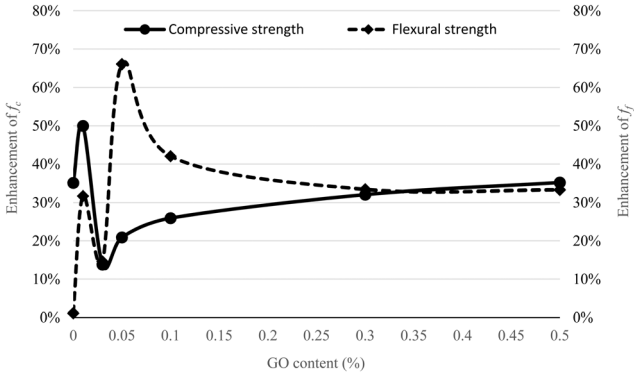


Fig. 8 The effect of GO on the development of strength from 7 to 28 days.

general increase is observed from 7 to 28 days when GO is added to the cement composites. The enhancement of compressive strength continues as the GO keeps growing. However, the flexural strength for GO decreases beyond 0.05 wt% cement content.

### 3.3. Transport properties

The apparent density and VPV of the cementitious composites are calculated and reported in Fig. 9. These two measurements are directly related to the structural integrity of cementitious binders and follow similar trends. The lowest density (2.09 g cm$^{-3}$) and VPV (23.44%) are related to the specimen containing 0.5% GO nanosheets in its composition. On the other hand, the highest values of density (2.617 g cm$^{-3}$) and VPV (29.47%) were found in the specimen with 0.03% GO by mass of cement. Additionally, the apparent density and VPV of GO-incorporated cement composites experience a vivid decrease when the GO content exceeds 0.03% by weight of cement.

The apparent density and VPV of cement binders, like UPV, depend upon the structural uniformity of the cementitious matrix. The predomination of factors impacting this uniformity can regulate the density and VPV of cement composites. Proof of the statement can be sought in Fig. 9, where the apparent density and VPV of GO-incorporated cement composites follow a very similar trend. Water sorptivity also is a function of structural integrity and void distribution. GO nanoflakes may

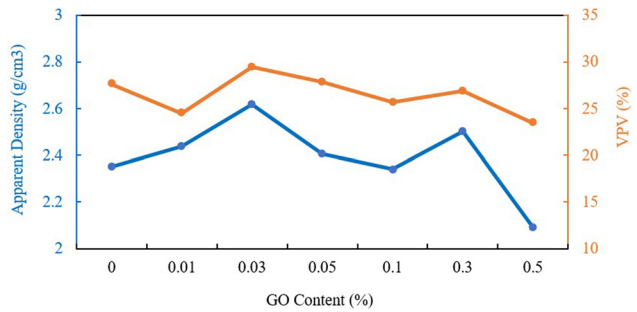


Fig. 9 Apparent density and VPV changes in GO-incorporated cement mortars.

 © 2022 The Author(s). Published by the Royal Society of Chemistry

Open Access Article. Published on 20 October 2022. Downloaded on 1/18/2026 10:53:13 AM.
This article is licensed under a Creative Commons Attribution-NonCommercial 3.0 Unported Licence.

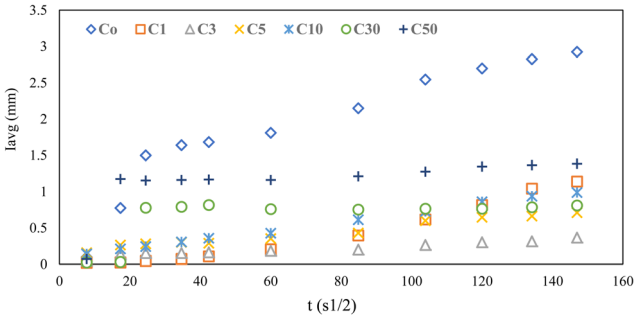


Fig. 10 Initial water absorption rate of specimens.

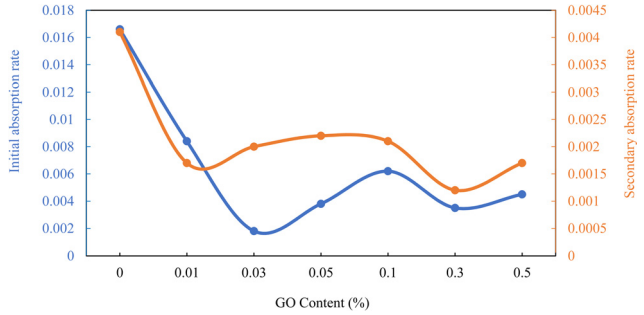


Fig. 12 Evaluation of water sorptivity rate as a function of GO content.

affect these factors in two contradictory ways. The addition of GO increases the homogeneity of the matrix by providing suitable (high energy) nucleation sites for the precipitation of calcium silicate hydrate products. It is worth mentioning that factors such as the initial setting time, temperature, density and saturation of CSH products, the Lucas–Washburn function of capillary transport, and diffusing ion capacity have effects on GO's extent of impact.[109–111] The reduction of the setting time, which influences the flowability consequently, results in the creation of more air voids in the hardened structure, leading to a high sorptivity rate. The governance of each of these parameters can describe the water absorption rate of GO-incorporated cement composites.

For the water sorptivity test, the initial (*i.e.*, first six hours) and secondary (*i.e.*, seven days) water absorptions were measured, followed by regression analysis of the recorded values. As a result, the initial and secondary absorption rates can be calculated by plotting average absorption ($I$) as the dependent variable *versus* the square root of time ($t^{1/2}$). Fig. 10 and 11 illustrate the changes in water absorption during the first six hours and seven days.

Fig. 10 and 11 show that the specimen without GO showed a vividly higher absorption rate both in the initial and secondary stages. The average absorption experienced a minimum of 50% reduction in GO-incorporated mortars (*i.e.*, C50 in the first six hours and C10 in seven days). Furthermore, the increase in the water sorptivity of C0 had a steeper trend compared to GO-incorporated specimens, especially in the initial stage. This shows the existence of a more uniform and homogenous microstructure upon the addition of GO.

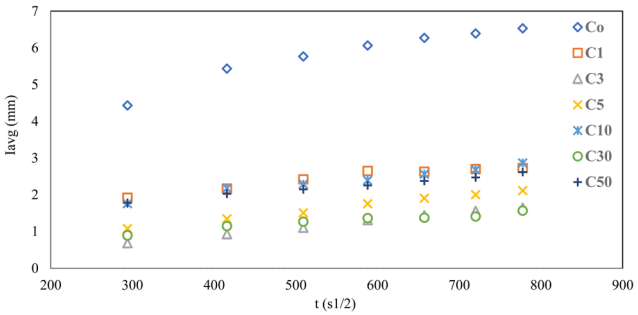


Fig. 11 Secondary water absorption rate of specimens.

Accordingly, Fig. 12 evaluates the initial and secondary rates of water absorption of cement composites based on the GO content. Fig. 12 simply shows that the initial and secondary water absorption rates of GO-reinforced cement composites fluctuate similarly, depending on the GO percentage. Generally, incorporating GO nanoplate reduces the water absorption of the cement binder. However, this reduction stops after addition of a certain amount of GO, which is 0.03% for the initial stage and 0.01 for the secondary stage.

Analysing the initial and secondary water absorption over time and GO content, as presented in Fig. 10–12, show the improvement in the durability of cement mortars by using GO. The inclusion of GO reduced the initial and secondary rates of water sorptivity up to 88% and 66%, respectively. The specimen with 0.03% GO content showed the best performance among the specimens in the initial absorption rate, which was in agreement with previous findings as well.[1] Despite the strong decline of the initial rate in the 0.03% specimen, specimens with higher GO contents (*i.e.*, 0.1%, 0.3% and 0.5%) showed less fluctuations in initial and secondary absorption rate, indicating a more uniform microstructure.

## 4. Conclusions

Graphene oxide is one of the solutions introduced to respond to the need for stronger, more durable concrete. This research attempted to investigate the impacts of adding GO to cement mortars on fresh physical, mechanical and transport properties by a more unified approach with a wider range of GO inclusion. The findings and results of this study indicated the followings:

1. The introduction of GO to cementitious composites can result in the reduction of setting time and workability due to the presence of more nucleation sites with a higher heat of hydration and unavailability of free water in the matrix. The highest impacts were witnessed in specimens with 0.05 wt% GO for the initial setting time and 0.03 wt% GO for flowability, as they reduced the mentioned properties by 23% and 31%, respectively.

2. The reduction of free water due to the incorporation of GO leads to the increase of electrical resistivity of the mortars, which is a beneficial advantage for concrete durability. However, adding excessive amounts of GO can negatively impact the resistivity of specimens as the decreasing trend of adding 0.1 wt

Open Access Article. Published on 20 October 2022. Downloaded on 1/18/2026 10:53:13 AM. This article is licensed under a Creative Commons Attribution-NonCommercial 3.0 Unported Licence.

and more. The UPV test findings indicate that the cementitious composites' homogeneity and uniformity remain stable and intact with the incorporation of more than 0.01% GO.

3. The inclusion of GO leads to an increase in the compressive and flexural strength of cement composites. The results illustrate a 17–46% increase in 7 day and 7–28% in 28 day compressive strength. The flexural strength results, however, indicate that the full development of flexural strength occurs in a longer term. The 7 day strength for the specimens was lower than the control specimen, but an increase of 28–50% was witnessed after 28 days. Despite achieving the highest compressive strength, the flexural performance of the specimen with 0.5 wt% GO inclusion was almost similar to that of the control specimen.

4. The transport properties of cement composites as an indicator of durability behaviour exhibited an enhancement with the introduction of GO to the mortar. The significant reduction in initial and secondary water absorption rate and sorptivity led to the conclusion that GO incorporation can positively impact the microstructure of cement mortars. The fluctuations of VPV and sorptivity results indicate that the transport properties of cement composites are highly dependent on the amount of GO content, and higher volumes of GO (*i.e.*, 0.1% and more) can reduce the porosity and voids of the microstructure and water sorptivity more effectively.

## Conflicts of interest

There are no conflicts to declare.

## Acknowledgements

The authors acknowledge the support from the Swinburne University of Technology for providing the opportunity to conduct this research.

## References

1 A. Mohammed, *et al.*, Incorporating graphene oxide in cement composites: A study of transport properties, *Constr. Build. Mater.*, 2015, **84**, 341–347.
2 C. S. R. Indukuri and R. Nerella, Enhanced transport properties of graphene oxide based cement composite material, *J. Build. Eng.*, 2021, **37**, 102174.
3 G. F. Huseien, K. W. Shah and A. R. M. Sam, Sustainability of nanomaterials based self-healing concrete: An all-inclusive insight, *J. Build. Eng.*, 2019, **23**, 155–171.
4 L. Aljerf, Effect of thermal-cured hydraulic cement admixtures on the mechanical properties of concrete, *Inter-Ceram: Int. Ceram. Rev.*, 2015, **64**(8), 346–356.
5 M. Balapour, A. Joshaghani and F. Althoey, Nano-$SiO_2$ contribution to mechanical, durability, fresh and micro-structural characteristics of concrete: A review, *Constr. Build. Mater.*, 2018, **181**, 27–41.
6 Y. L. Yaphary, *et al.*, Mechanical properties of colloidal calcium-silicate-hydrate gel with different gel-pore ionic solutions: A mesoscale study, *Microporous Mesoporous Mater.*, 2021, **316**, 110944.
7 R. Tepfers, *Concrete technology–porosity is decisive*, Befestigungstechnik, Bewehrungstechnik und… II, ibidem-Verlag, 2012.
8 R. Kumar and B. Bhattacharjee, Porosity, pore size distribution and in situ strength of concrete, *Cem. Concr. Res.*, 2003, **33**(1), 155–164.
9 D. Hou, *et al.*, Statistical modelling of compressive strength controlled by porosity and pore size distribution for cementitious materials, *Cem. Concr. Compos.*, 2019, **96**, 11–20.
10 X. Chen, S. Wu and J. Zhou, Influence of porosity on compressive and tensile strength of cement mortar, *Constr. Build. Mater.*, 2013, **40**, 869–874.
11 S. Zhang, *et al.*, Influence of the porosity and pore size on the compressive and splitting strengths of cellular concrete with millimeter-size pores, *Constr. Build. Mater.*, 2020, **235**, 117508.
12 G. Quercia, *et al.*, SCC modification by use of amorphous nano-silica, *Cem. Concr. Compos.*, 2014, **45**, 69–81.
13 W. Li, *et al.*, Influence of nanolimestone on the hydration, mechanical strength, and autogenous shrinkage of ultrahigh-performance concrete, *J. Mater. Civ. Eng.*, 2016, **28**(1), 04015068.
14 G. Y. Li, P. M. Wang and X. Zhao, Mechanical behavior and microstructure of cement composites incorporating surface-treated multi-walled carbon nanotubes, *Carbon*, 2005, **43**(6), 1239–1245.
15 V. Achal, X. Pan and N. Özyurt, Improved strength and durability of fly ash-amended concrete by microbial calcite precipitation, *Ecol. Eng.*, 2011, **37**(4), 554–559.
16 T. Chen and X. Gao, Use of carbonation curing to improve mechanical strength and durability of pervious concrete, *ACS Sustainable Chem. Eng.*, 2020, **8**(9), 3872–3884.
17 H. Chao-Lung, B. Le Anh-Tuan and C. Chun-Tsun, Effect of rice husk ash on the strength and durability characteristics of concrete, *Constr. Build. Mater.*, 2011, **25**(9), 3768–3772.
18 N. K. Amudhavalli and J. Mathew, Effect of silica fume on strength and durability parameters of concrete, *Int. J. Eng. Sci. Emerging Technol.*, 2012, **3**(1), 28–35.
19 H. Xiao, *et al.*, Role of nano-$SiO_2$ in improving the micro-structure and impermeability of concrete with different aggregate gradations, *Constr. Build. Mater.*, 2018, **188**, 537–545.
20 P. O. Awoyera, A. Adesina and R. Gobinath, Role of recycling fine materials as filler for improving performance of concrete-a review, *Aust. J. Civ. Eng.*, 2019, **17**(2), 85–95.
21 L. Chaurasia, *et al.*, A novel approach of biomineralization for improving micro and macro-properties of concrete, *Constr. Build. Mater.*, 2019, **195**, 340–351.
22 P. A. Claisse, *Transport properties of concrete: Measurements and applications*, Elsevier, 2014.

 © 2022 The Author(s). Published by the Royal Society of Chemistry

Open Access Article. Published on 20 October 2022. Downloaded on 1/18/2026 10:53:13 AM.
This article is licensed under a Creative Commons Attribution-NonCommercial 3.0 Unported Licence.

23 F. Dabbaghi, *et al.*, Characterizing fiber reinforced concrete incorporating zeolite and metakaolin as natural pozzolans, *Structures*, 2021, **34**, 2617–2627.
24 S. S. Raza, *et al.*, Effect of different fibers (steel fibers, glass fibers, and carbon fibers) on mechanical properties of reactive powder concrete, *Struct. Concr.*, 2021, **22**(1), 334–346.
25 M. Nili and V. Afroughsabet, Combined effect of silica fume and steel fibers on the impact resistance and mechanical properties of concrete, *Int. J. Impact Eng.*, 2010, **37**(8), 879–886.
26 S. Iqbal, *et al.*, Enhanced mechanical properties of fiber reinforced concrete using closed steel fibers, *Mater. Struct.*, 2019, **52**(3), 56.
27 S. Chuah, *et al.*, Nano reinforced cement and concrete composites and new perspective from graphene oxide, *Constr. Build. Mater.*, 2014, **73**, 113–124.
28 M. Rizwan, *et al.*, Types and classification of nanomaterials, *Nanomaterials: Synthesis, Characterization, Hazards and Safety*, Elsevier, 2021, pp. 31–54.
29 A. Adesina, *Durability enhancement of concrete using nanomaterials: an overview*, Trans Tech Publ., 2019.
30 W. Li, *et al.*, Effects of nanoparticle on the dynamic behaviors of recycled aggregate concrete under impact loading, *Mater. Des.*, 2016, **112**, 58–66.
31 Z. Pan, *et al.*, Mechanical properties and microstructure of a graphene oxide–cement composite, *Cem. Concr. Compos.*, 2015, **58**, 140–147.
32 F. Sanchez and K. Sobolev, Nanotechnology in concrete–a review, *Constr. Build. Mater.*, 2010, **24**(11), 2060–2071.
33 L. G. Li, *et al.*, Combined usage of micro-silica and nano-silica in concrete: SP demand, cementing efficiencies and synergistic effect, *Constr. Build. Mater.*, 2018, **168**, 622–632.
34 P. P. Abhilash, *et al.*, Effect of nano-silica in concrete; a review, *Constr. Build. Mater.*, 2021, **278**, 122347.
35 D. Kong, *et al.*, Influence of nano-silica agglomeration on microstructure and properties of the hardened cement-based materials, *Constr. Build. Mater.*, 2012, **37**, 707–715.
36 H. Du, S. Du and X. Liu, Durability performances of concrete with nano-silica, *Constr. Build. Mater.*, 2014, **73**, 705–712.
37 A. Bahari, *et al.*, Synthesis and strength study of cement mortars containing sic nano particles, *Dig. J. Nanomater. Biostructures*, 2012, **7**(4), 1427–1435.
38 A. S. Nik and O. L. Omran, Estimation of compressive strength of self-compacted concrete with fibers consisting nano-$SiO_2$ using ultrasonic pulse velocity, *Constr. Build. Mater.*, 2013, **44**, 654–662.
39 M. A. Kafi, *et al.*, Microstructural characterization and mechanical properties of cementitious mortar containing montmorillonite nanoparticles, *J. Mater. Civ. Eng.*, 2016, **28**(12), 04016155.
40 A. Sadeghi-Nik, *et al.*, Modification of microstructure and mechanical properties of cement by nanoparticles through a sustainable development approach, *Constr. Build. Mater.*, 2017, **155**, 880–891.
41 M. Nili and A. Ehsani, Investigating the effect of the cement paste and transition zone on strength development of concrete containing nanosilica and silica fume, *Mater. Des.*, 2015, **75**, 174–183.
42 L. Aljerf and R. Nadra, Developed greener method based on MW implementation in manufacturing CNFs, *Int. J. Nanomanuf.*, 2019, **15**(3), 269–289.
43 J.-P. Salvetat, *et al.*, Elastic and shear moduli of single-walled carbon nanotube ropes, *Phys. Rev. Lett.*, 1999, **82**(5), 944.
44 X. Li, *et al.*, Co-effects of graphene oxide sheets and single wall carbon nanotubes on mechanical properties of cement, *J. Phys. Chem. Solids*, 2015, **85**, 39–43.
45 M.-F. Yu, *et al.*, Strength and breaking mechanism of multiwalled carbon nanotubes under tensile load, *Science*, 2000, **287**(5453), 637–640.
46 A. Peigney, *et al.*, Specific surface area of carbon nanotubes and bundles of carbon nanotubes, *Carbon*, 2001, **39**(4), 507–514.
47 A. Carriço, *et al.*, Durability of multi-walled carbon nanotube reinforced concrete, *Constr. Build. Mater.*, 2018, **164**, 121–133.
48 H. K. Kim, I. W. Nam and H.-K. Lee, Enhanced effect of carbon nanotube on mechanical and electrical properties of cement composites by incorporation of silica fume, *Compos. Struct.*, 2014, **107**, 60–69.
49 B. Zou, *et al.*, Effect of ultrasonication energy on engineering properties of carbon nanotube reinforced cement pastes, *Carbon*, 2015, **85**, 212–220.
50 M. Ramezani, A. Dehghani and M. M. Sherif, Carbon nanotube reinforced cementitious composites: A comprehensive review, *Constr. Build. Mater.*, 2022, **315**, 125100.
51 V. Vilela Rocha and P. Ludvig, Influence of carbon nanotubes on the mechanical behavior and porosity of cement pastes prepared by a dispersion on cement particles in isopropanol suspension, *Materials*, 2020, **13**(14), 3164.
52 A. Cwirzen, *et al.*, SEM/AFM studies of cementitious binder modified by MWCNT and nano-sized Fe needles, *Mater. Charact.*, 2009, **60**(7), 735–740.
53 M. Ramezani, Y. H. Kim and Z. Sun, Modeling the mechanical properties of cementitious materials containing CNTs, *Cem. Concr. Compos.*, 2019, **104**, 103347.
54 M. Ramezani, Y. H. Kim and Z. Sun, Mechanical properties of carbon-nanotube-reinforced cementitious materials: Database and statistical analysis, *Mag. Concr. Res.*, 2020, **72**(20), 1047–1071.
55 M. Ramezani, Y. H. Kim and Z. Sun, Probabilistic model for flexural strength of carbon nanotube reinforced cement-based materials, *Compos. Struct.*, 2020, **253**, 112748.
56 M. Ramezani, Y. H. Kim and Z. Sun, Elastic modulus formulation of cementitious materials incorporating carbon nanotubes: Probabilistic approach, *Constr. Build. Mater.*, 2021, **274**, 122092.
57 Y. Xu, *et al.*, A holistic review of cement composites reinforced with graphene oxide, *Constr. Build. Mater.*, 2018, **171**, 291–302.
58 D. Chen, H. Feng and J. Li, Graphene oxide: preparation, functionalization, and electrochemical applications, *Chem. Rev.*, 2012, **112**(11), 6027–6053.

Open Access Article. Published on 20 October 2022. Downloaded on 1/18/2026 10:53:13 AM.
This article is licensed under a Creative Commons Attribution-NonCommercial 3.0 Unported Licence.

59 Y. Gao, *et al.*, Influence of ultrasonication on the dispersion and enhancing effect of graphene oxide–carbon nanotube hybrid nanoreinforcement in cementitious composite, *Composites, Part B*, 2019, **164**, 45–53.
60 S. C. Ray, Application and uses of graphene oxide and reduced graphene oxide, *Applications of graphene and graphene-oxide based nanomaterials*, 2015, p. 1.
61 D. Hou, *et al.*, Reactive molecular simulation on water confined in the nanopores of the calcium silicate hydrate gel: structure, reactivity, and mechanical properties, *J. Phys. Chem. C*, 2015, **119**(3), 1346–1358.
62 S. Stankovich, *et al.*, Synthesis and exfoliation of isocyanate-treated graphene oxide nanoplatelets, *Carbon*, 2006, **44**(15), 3342–3347.
63 Z. Lu, *et al.*, Effects of graphene oxide on the properties and microstructures of the magnesium potassium phosphate cement paste, *Constr. Build. Mater.*, 2016, **119**, 107–112.
64 T. Kuilla, *et al.*, Recent advances in graphene based polymer composites, *Prog. Polym. Sci.*, 2010, **35**(11), 1350–1375.
65 E. Shamsaei, *et al.*, Graphene-based nanosheets for stronger and more durable concrete: A review, *Constr. Build. Mater.*, 2018, **183**, 642–660.
66 Y. Shang, *et al.*, Effect of graphene oxide on the rheological properties of cement pastes, *Constr. Build. Mater.*, 2015, **96**, 20–28.
67 X. Li, *et al.*, Effects of graphene oxide agglomerates on workability, hydration, microstructure and compressive strength of cement paste, *Constr. Build. Mater.*, 2017, **145**, 402–410.
68 K. Gong, *et al.*, Reinforcing effects of graphene oxide on portland cement paste, *J. Mater. Civ. Eng.*, 2015, **27**(2), A4014010.
69 Q. Wang, *et al.*, Rheological behavior of fresh cement pastes with a graphene oxide additive, *New Carbon Mater.*, 2016, **31**(6), 574–584.
70 C. Lin, W. Wei and Y. H. Hu, Catalytic behavior of graphene oxide for cement hydration process, *J. Phys. Chem. Solids*, 2016, **89**, 128–133.
71 L. Zhao, *et al.*, An intensive review on the role of graphene oxide in cement-based materials, *Constr. Build. Mater.*, 2020, **241**, 117939.
72 S. Lv, *et al.*, Effect of graphene oxide nanosheets of microstructure and mechanical properties of cement composites, *Constr. Build. Mater.*, 2013, **49**, 121–127.
73 E. Horszczaruk, *et al.*, Nanocomposite of cement/graphene oxide–Impact on hydration kinetics and Young's modulus, *Constr. Build. Mater.*, 2015, **78**, 234–242.
74 X. Li, *et al.*, Effects of graphene oxide aggregates on hydration degree, sorptivity, and tensile splitting strength of cement paste, *Composites, Part A*, 2017, **100**, 1–8.
75 W.-J. Long, *et al.*, Microstructure development and mechanism of hardened cement paste incorporating graphene oxide during carbonation, *Cem. Concr. Compos.*, 2018, **94**, 72–84.
76 M. Wang, *et al.*, Study on the three dimensional mechanism of graphene oxide nanosheets modified cement, *Constr. Build. Mater.*, 2016, **126**, 730–739.
77 T. S. Qureshi and D. K. Panesar, Impact of graphene oxide and highly reduced graphene oxide on cement based composites, *Constr. Build. Mater.*, 2019, **206**, 71–83.
78 J. He, *et al.*, Laboratory investigation of graphene oxide suspension as a surface sealer for cementitious mortars, *Constr. Build. Mater.*, 2018, **162**, 65–79.
79 W.-J. Long, *et al.*, Inhibited effect of graphene oxide on calcium leaching of cement pastes, *Constr. Build. Mater.*, 2019, **202**, 177–188.
80 S. C. Devi and R. A. Khan, Effect of graphene oxide on mechanical and durability performance of concrete, *J. Build. Eng.*, 2020, **27**, 101007.
81 I. De la Varga, *et al.*, Fluid transport in high volume fly ash mixtures with and without internal curing, *Cem. Concr. Compos.*, 2014, **45**, 102–110.
82 W. P. S. Dias, Reduction of concrete sorptivity with age through carbonation, *Cem. Concr. Res.*, 2000, **30**(8), 1255–1261.
83 S. Zhang and L. Zong, Evaluation of relationship between water absorption and durability of concrete materials, *Adv. Mater. Sci. Eng.*, 2014, **2014**, DOI: 10.1155/2014/650373.
84 C. Hall, Water sorptivity of mortars and concretes: a review, *Mag. Concr. Res.*, 1989, **41**(147), 51–61.
85 T. Ji, Preliminary study on the water permeability and microstructure of concrete incorporating nano-$SiO_2$, *Cem. Concr. Res.*, 2005, **35**(10), 1943–1947.
86 W. Li, *et al.*, Effects of graphene oxide on early-age hydration and electrical resistivity of Portland cement paste, *Constr. Build. Mater.*, 2017, **136**, 506–514.
87 X. Li, *et al.*, Incorporation of graphene oxide and silica fume into cement paste: A study of dispersion and compressive strength, *Constr. Build. Mater.*, 2016, **123**, 327–335.
88 M. Saafi, *et al.*, Enhanced properties of graphene/fly ash geopolymeric composite cement, *Cem. Concr. Res.*, 2015, **67**, 292–299.
89 A. Standards, AS 3972-General purpose and blended cement, Standards Australia, NSW, Australia, 2010, p. 29.
90 M. Hadadian, E. K. Goharshadi and A. Youssefi, Electrical conductivity, thermal conductivity, and rheological properties of graphene oxide-based nanofluids, *J. Nanopart. Res.*, 2014, **16**(12), 1–17.
91 International, A., *ASTM C1437-20, Standard Test Method for Flow of Hydraulic Cement Mortar*, ASTM International, West Conshohocken, PA, 2020.
92 International, A., *ASTM C191-19, Standard Test Methods for Time of Setting of Hydraulic Cement by Vicat Needle*, ASTM International, West Conshohocken, PA, 2019.
93 Z. Yi, *et al.*, Detection of setting time in cement hydration using patch antenna sensor, *Struct. Control Health Monit.*, 2022, **29**(1), e2855.
94 G. Karaiskos, *et al.*, Monitoring of concrete structures using the ultrasonic pulse velocity method, *Smart Mater. Struct.*, 2015, **24**(11), 113001.
95 Internatioal, A., *ASTM C597-16, Standard Test Method for Pulse Velocity Through Concrete*, ASTM International: Conshohocken, PA, 2016.
96 Internatioal, A., *ASTM C1876-19, Standard Test Method for Bulk Electrical Resistivity or Bulk Conductivity of Concrete*, ASTM International: Conshohocken, PA, 2019.
97 L. Coppola, *et al.*, Chloride diffusion in concrete protected with a silane-based corrosion inhibitor, *Materials*, 2020, **13**(8), 2001.

 © 2022 The Author(s). Published by the Royal Society of Chemistry

Open Access Article. Published on 20 October 2022. Downloaded on 1/18/2026 10:53:13 AM.
This article is licensed under a Creative Commons Attribution-NonCommercial 3.0 Unported Licence.

98 ASTM International, *ASTM C39/C39M-21, Standard Test Method for Compressive Strength of Cylindrical Concrete Specimens*, ASTM International: West Conshohocken, PA, 2021.

99 International, A., *ASTM C348-21, Standard Test Method for Flexural Strength of Hydraulic-Cement Mortars*, ASTM International: West Conshohocken, PA, 2021.

100 International, A., *ASTM C1585-20, Standard Test Method for Measurement of Rate of Absorption of Water by Hydraulic-Cement Concretes*, ASTM International: West Conshohocken, PA, 2020.

101 Internation, A., *ASTM C642-13, Standard Test Method for Density, Absorption, and Voids in Hardened Concrete*, ASTM International: Conshohocken, PA, 2013.

102 W. Li, *et al.*, Effects of nanoalumina and graphene oxide on early-age hydration and mechanical properties of cement paste, *J. Mater. Civ. Eng.*, 2017, **29**(9), 04017087.

103 K. Chintalapudi and R. M. R. Pannem, The effects of Graphene Oxide addition on hydration process, crystal shapes, and microstructural transformation of Ordinary Portland Cement, *J. Build. Eng.*, 2020, **32**, 101551.

104 M. Newell and E. Garcia-Taengua, Fresh and hardened state properties of hybrid graphene oxide/nanosilica cement composites, *Constr. Build. Mater.*, 2019, **221**, 433–442.

105 H. N. Catherine, *et al.*, Adsorption mechanism of emerging and conventional phenolic compounds on graphene oxide nanoflakes in water, *Sci. Total Environ.*, 2018, **635**, 629–638.

106 X. Li, *et al.*, Dispersion of graphene oxide agglomerates in cement paste and its effects on electrical resistivity and flexural strength, *Cem. Concr. Compos.*, 2018, **92**, 145–154.

107 H. Zeng, *et al.*, Effect of graphene oxide on permeability of cement materials: An experimental and theoretical perspective, *J. Build. Eng.*, 2021, **41**, 102326.

108 R. Gopalakrishnan and R. Kaveri, Using graphene oxide to improve the mechanical and electrical properties of fiber-reinforced high-volume sugarcane bagasse ash cement mortar, *Eur. Phys. J. Plus*, 2021, **136**(2), 1–15.

109 D. Hou, *et al.*, Modified Lucas-Washburn function of capillary transport in the calcium silicate hydrate gel pore: A coarse-grained molecular dynamics study, *Cem. Concr. Res.*, 2020, **136**, 106166.

110 J. Yu, *et al.*, Insights on the capillary transport mechanism in the sustainable cement hydrate impregnated with graphene oxide and epoxy composite, *Composites, Part B*, 2019, **173**, 106907.

111 H. Yang, *et al.*, Experimental study of the effects of graphene oxide on microstructure and properties of cement paste composite, *Composites, Part A*, 2017, **102**, 263–272.